PHYSICAL REVIEW E VOLUME 58, NUMBER 5 NOVEMBER 1998

Role of the plasma scale length in the harmonic generation from solid targets

M. Zepf,[1] G. D. Tsakiris,[2] G. Pretzler,[2] I. Watts,[1] D. M. Chambers,[3] P. A. Norreys,[4] U. Andiel,[2] A. E. Dangor,[1] K. Eidmann,[2] C. Gahn,[2] A. Machacek,[3] J. S. Wark,[3] and K. Witte[2]

[1]*Blackett Laboratory, Imperial College of Science, Technology and Medicine, London SW7 2AZ, United Kingdom*

[2]*Max-Planck-Institut für Quantenoptik, D-85748 Garching, Germany*

[3]*Clarendon Laboratory, Department of Physics, University of Oxford, Parks Road, Oxford OX1 3PU, United Kingdom*

[4]*Central Laser Facility, Rutherford Appleton Laboratory, Chilton, Didcot, Oxon OX11 0QX, United Kingdom*

(Received 1 April 1998; revised manuscript received 9 July 1998)

We have investigated the generation of high harmonics from the interaction of 150 fsec, 790 nm, and 395 nm laser pulses with solid targets. Experiments are presented that demonstrate a strong dependence of the conversion efficiency on the temporal pulse shape and the resulting density scale length (L/λ) of the preformed plasma. The highest conversion efficiencies are achieved for short density scale lengths ($L/\lambda \leqslant 0.4$), which result from high contrast ratio pulse interactions. [S1063-651X(98)50211-5]

PACS number(s): 52.40.Nk, 42.65.Ky, 52.25.Qt, 52.35.Mw

Developments in short pulse laser technology have rekindled the interest in harmonic generation from solid targets, first observed with nanosecond pulses of long wavelength (10.6 μm) CO_2 laser light [1]. The subject has recently received considerable attention [2–9], not least due to spectacular predictions [10] for the overall conversion efficiency achievable at very short primary wavelengths. Indeed, particle-in-cell (PIC) simulations suggest that at irradiance values of $I\lambda^2 = 10^{19}$ W μm^2/cm^2 very high harmonic orders (>60) with conversion efficiencies $>10^{-6}$ are generated [10–12]. This is a very favorable wavelength scaling, as the conversion into a given order remains constant for a given value of $I\lambda^2$. It opens the possibility of extremely short wavelength xuv emission being generated with powerful uv drive lasers [9]. Qualitatively, the harmonic emission from solids can be understood in terms of the fundamental light being reflected in a steep density profile off the oscillating critical density surface [12–14].

In experiments with solid targets using laser pulses of picoseconds duration at $I\lambda^2 = 10^{19}$ W μm^2/cm^2, very high-order harmonics were observed (up to 75) at conversion efficiencies, which were in good quantitative agreement with PIC calculations for steep density gradients. The conversion efficiency was found to be independent of the prepulse level over a large range. This strongly suggests that the ponderomotive pressure, applied over the relatively long pulse length, generated the necessary steep density scale lengths ($L/\lambda \leqslant 0.2$) during the pulse itself, as was the interpretation for the nanosecond CO_2 experiments [1]. Measurements of the other source parameters [4,5] showed an isotropic angular distribution and a relatively large fractional bandwidth ($\Delta\lambda/\lambda \sim 10^{-2}$). This is quite a significant deviation from theoretical expectations, which suggest that the harmonic radiation should be reflected in the specular direction and with near transform-limited bandwidth. Results by Bulanov *et al.* [15] suggest that high-power laser pulses can be spectrally broadened by self-phase modulation in the preformed plasma. Indeed, observations by Zhang *et al.* [5] showed bandwidth broadening in good agreement with Bulanov *et al.* [15] and also an isotropic angular distribution. The latter was attributed to Rayleigh-Taylor-like surface rippling [16] and distortions due to the ponderomotive pressure [17], as the density profile is locally steepened at the critical surface. Furthermore, the strong critical surface rippling was also invoked to explain the not measurable difference in harmonic yield between *s* and *p* polarization of the laser beam [4], which is also in contradiction to the theoretical predictions [10,11].

A possible remedy is to use a high-intensity femtosecond laser pulse. This reduces the time for any critical surface instabilities and modulations to appear and can lead to the formation of very steep density gradients with no need for additional steepening processes [18]. In contrast to the picosecond results cited earlier, even in the early experiments with femtosecond laser pulses [2] it became apparent that, in this case, the *cleanness* of the pulse, i.e., the intensity contrast ratio, plays a decisive role in the generation of the harmonics. This is presumably due to the short pulse duration preventing significant ponderomotive steepening during the pulse itself. Thus, the harmonic generation process becomes far more dependent upon the plasma conditions imparted by the prepulse, since the scale length is mainly determined by the timespan between the onset of plasma formation and the peak of the pulse. However, no detailed study of the effects of prepulse in these femtosecond experiments has yet been reported. It is therefore timely to study the effect of the plasma existing before the peak of the pulse and devise ways of controlling its detrimental influence.

In this Rapid Communication, we present a detailed investigation of the effect of the pulse shape on the harmonic conversion efficiency for femtosecond pulses. We show that the harmonic efficiency does indeed depend strongly on the density scale length L/λ. We find qualitative agreement with PIC calculations when realistic density scale lengths, derived from hydrodynamic simulations and measured pulse shapes, are used.

The experiment was conducted using the Ti:sapphire ATLAS laser at the Max-Planck-Institut für Quantenoptik. It produces 150-fs, 200-mJ pulses at a repetition rate of 10 Hz at 790 nm. The laser intensity contrast ratio was measured on a routine basis by a second order autocorrelator in the ± 3 ps time window and it was found to be $1:10^3$ at 1ps (see

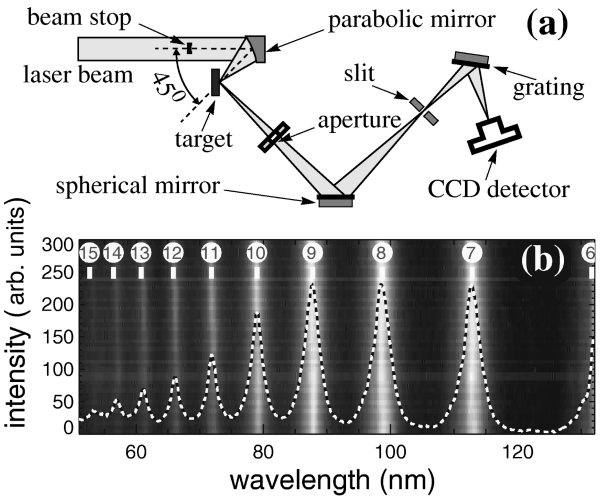

FIG. 1. (a) Schematic diagram of the experimental setup. (b) Single shot harmonic spectrum for 2.5×10^{18} W/cm^2 and a pulse contrast of $1{:}10^3$ at 1ps (dashed line: integrated lineout). The spectrum has not been corrected for the spectral response of the detection system.

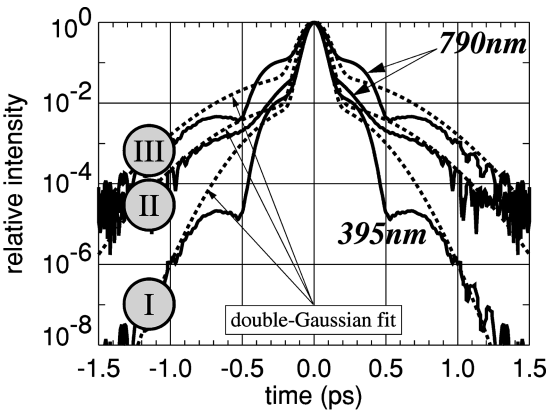

FIG. 2. Temporal pulse shape for the two low-contrast cases II and III, 790-nm pulses and the high-contrast case I, 395-nm pulses. The 790-nm pulse shapes are inferred from autocorrelation measurements assuming a symmetrical pulse in time. The 395-nm pulse in case I was produced by frequency doubling the pulse in case III. Its pulse shape is estimated from $I_{(395)}\sim I^2_{(790)}$ (see Ref. [19]). The dashed curves are double-Gaussian fits to the corresponding pulse shapes used as input to the hydrodynamic calculations.

Fig. 2). The prepulse from 30–2 ns before the main pulse was monitored using photodiodes with differential attenuation. The intensity contrast in this time window was better than $1{:}10^7$ with the exemption of a prepulse at 10^{-6} level 5 ns before the main pulse. For parts of the experiment, the laser was frequency doubled in a 4-mm-thick KD*P crystal. This resulted in 60 mJ at 395 nm in approximately the same pulse duration. The infrared was rejected by passing the beam over four dielectric coated mirrors. This increased the contrast ratio to $\sim1{:}10^6$ at 1 ps and to $>1{:}10^{10}$ in the 30–2 ns time window. The laser was focused using an $f/2.5$ diamond turned, off-axis parabola producing a focal spot of 4 μm full width at half maximum (FWHM) in diameter. The peak focused intensity was 2.5×10^{18} W/cm^2 for the fundamental and 5×10^{17} W/cm^2 at 395 nm.

As it is schematically shown in Fig. 1(a), the laser was incident onto an optically polished glass flat target at 45°, which was rotated between shots. The specularly reflected radiation was collected by a 5 cm diameter, 45° spherical focusing mirror coated with gold and imaged onto the entrance slit of an *Acton* vacuum spectrometer with a 1200 ℓ/mm iridium coated grating. The dispersed radiation was then detected with double microchannel plate detector in chevron configuration in the 160- to 40-nm spectral range. The data were digitized using a charge-coupled-device (CCD) detector. The harmonic radiation generated using a single shot from the ATLAS laser is shown in Fig. 1(b). It is seen that the harmonic emission is sufficiently intense to be clearly visible above the time-integrated plasma background. Therefore, all the data presented here were taken on single shots. The highest harmonics observed on a single shot basis was the 16th harmonic of the fundamental at 49.4 nm and the seventh harmonic of the frequency doubled beam at 56.4 nm. This is in good agreement with previous observations for similar values of $I\lambda^2$ [3,4].

Most of conclusions drawn in this Rapid Communication are based on the comparison of the $I\lambda^2$ scaling of the relative harmonic conversion efficiency for three distinct cases. One high-contrast case in which the laser was frequency doubled to $\lambda=395$ nm [19], case I, and two low-contrast cases which pertain to irradiation at the fundamental wavelength ($\lambda=790$ nm, cases II and III). The two low-contrast cases distinguish themselves in the exact temporal profile of the laser pulse resulting from a slightly different grating setting in the pulse compressor unit of the laser system. The temporal pulse shape in the time window of ±1.5 ps for the three cases is given in Fig. 2. The intensity contrast ratio decreases progressively from case I to case III. The development of the preplasma for the high- and low-contrast cases was calculated using the modified hydrocode MULTI-FS [20]. A double Gaussian fit to the temporal pulse shape was used for each case (see Fig. 2) and an estimate of the prevailing scale length before the arrival of the high intensity pulse was obtained. It was found that at 150 fs before the maximum of the laser pulse the high-contrast case I exhibits a scale length of $L/\lambda\approx0.2$ at maximum intensity. For the two low-contrast cases (II and III), scale lengths of $L/\lambda\approx0.4$ and $L/\lambda\approx0.8$ were obtained at a peak irradiance of 8.2×10^{17} Wμm^2/cm^2 and 1.6×10^{18} Wμm^2/cm^2, respectively. This represents a lower bound for the scale length in the low-contrast cases, as the exact pulse shape at the plasma formation intensity threshold could not be measured with the available diagnostics. There is also an uncertainty in the estimate because two-dimensional effects are not included in the simulation.

The effect of this scale length difference was investigated in a series of 1D PIC simulations performed using the LPIC code [21]. The density scale length here is defined according to the relation $n_e=n_c x/L$, where n_c is the critical density of the incident wave and x is the space coordinate perpendicular to the target surface. The incident irradiance was varied between 5.5×10^{16} W μm^2/cm^2 to 2.1×10^{18} W μm^2/cm^2 and the scale length of the density ramp between 0 and 3λ. The angle of incidence ($\theta_i=45°$) and polarization (p) were chosen to reflect the experimental conditions. The dependence of the harmonic efficiency $\eta_q=F(I\lambda^2,L/\lambda)$

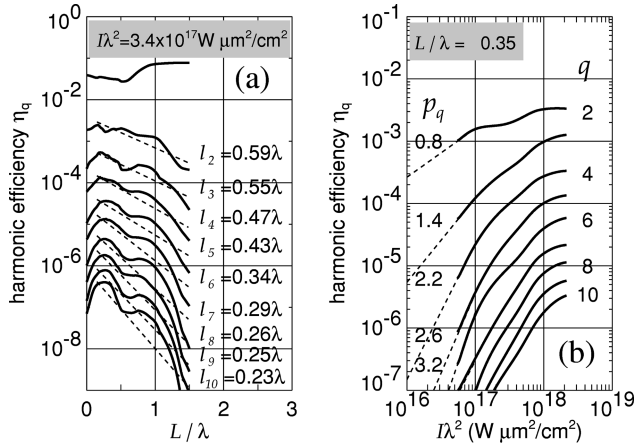

FIG. 3. (a) Variation of the harmonic efficiency η_q with the density scale length L/λ of the preformed plasma. The reduction of the efficiency with scale length is seen to be approximately exponential $\eta_q \sim e^{-L/l_q}$ (dashed lines). (b) Calculated $I\lambda^2$ scaling of several harmonics for $L/\lambda = 0.35$. The dashed lines represent the dependence $\eta_q \sim (I\lambda^2)^{p_q}$ for $I\lambda^2 < 10^{17}$ W μm^2/cm^2.

with respect to the laser irradiance and the density scale length was thus studied. A sample of it is depicted in Fig. 3.

As seen in Fig. 3(b), within a sufficiently small intensity interval, the efficiency of the qth harmonic scales approximately as $\eta_q \sim (I\lambda^2)^{p_q}$, where p_q is the effective nonlinearity associated with the qth harmonic [10,12]. The exact value p_q for a fixed density scale length depends weakly on $I\lambda^2$. Also, Fig. 3(a) shows clearly that all harmonics exhibit a maximum for an optimum value of $L/\lambda \approx 0.2-0.5$ [11] and then fall off approximately exponentially. This behavior can be understood in terms similar to resonance absorption [22]. For 45° angle of incidence, the optimum scale length for maximum conversion into the electrostatic mode is $L/\lambda \approx 0.23$. The plasma waves excited at the critical density surface decrease exponentially with increasing scale length, due to the increased distance between the turning point of the *p*-polarized light and the critical density surface. This, in turn, leads to the observed exponential drop in the harmonic efficiency. Very large values of L/λ should therefore make the harmonics unobservable. This was confirmed in our experiments by inserting a prepulse at 10^{-2} of the peak intensity ≈ 5 ps ahead of the peak of the pulse. No harmonic emission was observed in this case.

The polarization of the laser pulse was rotated by 90° so that *s*-polarized light was incident on target. In this case, the only harmonic observable above background was the third harmonic of the $\lambda = 790$ nm fundamental radiation. The efficiency of the third harmonic was measured to be three orders of magnitude lower than for *p*-polarized light. This is in agreement with PIC code predictions [11] and in sharp contrast to the results obtained with picosecond pulses [4]. That the angular distribution was concentrated in the specular direction was confirmed by placing a toroidal mirror at 32° degrees to the specular direction and directing the radiation into the *Acton* spectrometer. For *p*-polarized light, a two orders of magnitude reduction in high harmonic intensity was obtained. These measurements indicate that the experimental pulse parameters (i.e., the pulse duration, intensity, and focal spot size) were sufficient to prevent significant rippling and/or curvature of the critical density surface.

A comparison of the experimental data for the high-contrast case I and the calculated intensity scaling for $L/\lambda = 0.2$ is shown in Fig. 4. Clearly, there is excellent agreement between the simulation for a single density gradient ($L/\lambda = 0.2$) and the experiment over a large range of intensities for the harmonic orders investigated. This is to be expected when using a pulse with such a large contrast ratio. Increasing the peak intensity only has a small influence on the time of onset of plasma formation in this case and subsequently on the density scale length.

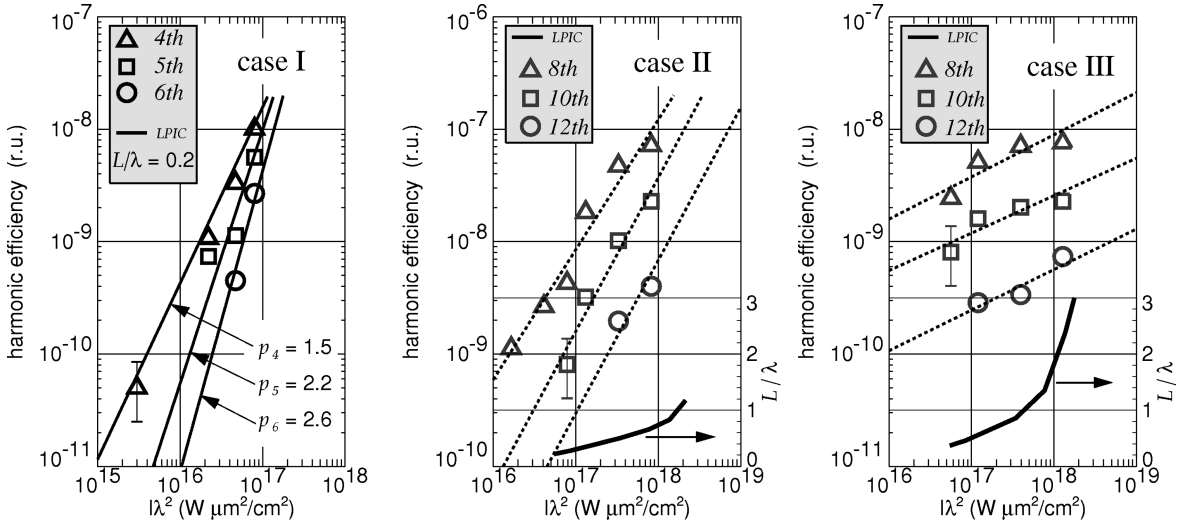

FIG. 4. $I\lambda^2$ scaling of the harmonic conversion efficiency in the same relative units for all of the three cases considered. The points are the experimental results for the indicated harmonics (see insets), and the error bars represent the shot-to-shot variation for all points. The data in case II (taken with a different experimental setup) have been normalized so that the data point for the tenth harmonic at 8.0×10^{16} W μm^2/cm^2 is the same with that of case III. Case I: the solid lines give the slope of the scaling predicted by the LPIC code for a fixed scale length of $L/\lambda = 0.2$ [see Fig. 2(b)]. Cases II and III: the dotted lines are power law fits to the experimental points, and the solid lines represent the scale length variation for which the LPIC code reproduces the experimentally observed scaling, i.e., the dotted lines.

However, the situation for the lower-contrast cases II and III is somewhat different. The experimental data cannot be fitted by the intensity scaling for a single value of L/λ. In the low-contrast cases, the time from the onset of plasma formation to the peak of the pulse depends strongly on the peak intensity. Therefore, the scale length of the plasma increases with increasing intensity. This reduces the apparent $I\lambda^2$ scaling of the harmonic efficiency, because the rise in conversion efficiency due to the increase in intensity is offset by the fall due to the increasing scale length. Figure 4 shows several harmonic orders plotted against incident irradiances for the two different low-contrast experimental runs. By requiring that the increase in harmonic intensity with increasing irradiation reproduces the slope exhibited experimentally (here approximated by a power law fit), one can deduce the corresponding scale length using the LPIC simulation results. The density scale length for the lowest intensity values can be calculated because the pulse shape near the plasma formation threshold is known (see Fig. 2). The variation of the scale length with increasing intensity for the two low-contrast cases is shown in Fig. 4. The observed increase reflects the fact that the onset of plasma formation moves earlier in time thus more time is available for longer density scale lengths to develop via hydrodynamic expansion. The density scale lengths at peak intensity inferred from the irradiance dependence are by a factor of ~ 2 larger than those obtained through hydrodynamic calculations. This is to be expected since, as pointed out previously, the exact pulse shape at plasma formation threshold was not known. It is interesting to note that the cases I and III within the error bars show very similar conversion efficiencies for the neighboring sixth harmonic of 395 nm and the eight harmonic of 790 nm for the value of $I\lambda^2 \sim 10^{17}$ W μm^2/cm^2 for which the plasma scale length is approximately the same. This is experimental evidence that the conversion efficiency does indeed scale with wavelength as suggested by theoretical results [10].

In conclusion, we have investigated the effects of prepulse on harmonics generated from intense femtosecond laser-solid interactions. We have presented three cases which in a striking manner show the close correspondence between degree of pulse *cleanness* and higher value of nonlinearity associated with the $I\lambda^2$ scaling of the harmonic efficiency. In doing so, we have demonstrated that the efficiency of xuv harmonics from solid targets, for the case of femtosecond pulses over the range of $I\lambda^2$ investigated, depends very sensitively on the density scale length of the plasma and subsequently on the prepulse and pedestal level of the driving laser. In general, the lower the contrast of the laser pulse the weaker the $I\lambda^2$ scaling of the harmonic conversion efficiency. It is therefore necessary, at least for the intensities and pulse duration used in these experiments, to use very high-contrast ratio lasers to exploit the extremely promising theoretical predictions for this source of xuv radiation.

The authors gratefully acknowledge the support of the ATLAS laser staff at MPQ and the assistance by R. E. W. Pfund and R. Lichters in running the LPIC code. The experiment was funded by the EC HCM Program under Contract No. ERB CHGE CT92 0006. Four of us (D.M.C., A.M., M.Z., and I.W.) would like to acknowledge financial support from EPSRC.

[1] R. L. Carman *et al.*, Phys. Rev. Lett. **49**, 202 (1981).
[2] S. Kohlweyer *et al.*, Opt. Commun. **177**, 431 (1995).
[3] D. von der Linde *et al.*, Phys. Rev. A **52**, R25 (1995).
[4] P. A. Norreys *et al.*, Phys. Rev. Lett. **76**, 1832 (1996).
[5] J. Zhang *et al.*, Phys. Rev. A **54**, 1597 (1996).
[6] I. B. Földes *et al.*, IEEE J. Sel. Top. Quantum Electron. **2**, 776 (1996).
[7] D.M. Chambers *et al.*, J. Appl. Phys. **81**, 2055 (1997).
[8] P. Gibbon, IEEE J. Quantum Electron. **33**, 1915 (1997).
[9] D. M. Chambers *et al.*, Opt. Commun. **148**, 289 (1998).
[10] P. Gibbon, Phys. Rev. Lett. **76**, 50 (1996).
[11] R. Lichters *et al.*, Inst. Phys. Conf. Ser. **154**, 221 (1997).
[12] R. Lichters *et al.*, Phys. Plasmas **3**, 3425 (1996).
[13] D. von der Linde *et al.*, Appl. Phys. B: Lasers Opt. **63**, 499 (1996).
[14] S. V. Bulanov *et al.*, Phys. Plasmas **1**, 745 (1994).
[15] S. V. Bulanov *et al.*, Phys. Scr. **T63**, 258 (1996).
[16] S. C. Wilks *et al.*, Phys. Rev. Lett. **69**, 1383 (1992).
[17] R. Fedosejevs *et al.*, Phys. Fluids **24**, 537 (1981).
[18] S. Bastiani *et al.*, Phys. Rev. E **56**, 7179 (1997).
[19] D. F. Price *et al.*, Phys. Rev. Lett. **75**, 252 (1995).
[20] R. Ramis *et al.*, Comput. Phys. Commun. **49**, 475 (1988).
[21] R. Lichters *et al.*, MPQ Report No. 225, 1997 (unpublished).
[22] L. A. Gizzi *et al.*, Phys. Rev. Lett. **76**, 2278 (1996).